Understanding the Nature of the Molecular Mechanisms Associated with the Competitive Lewis Acid Catalyzed [4+2] and [4+3] Cycloadditions between Arylidenoxazolone Systems and Cyclopentadiene: A DFT Analysis

Manuel Arnó,[a] M. Teresa Picher,[a] Luis R. Domingo,*[a] and Juan Andrés[b]

Abstract: The molecular mechanisms of the reactions between arylidene-5(4*H*)-oxazolone **1**, and cyclopentadiene (**Cp**), in presence of Lewis acid (LA) catalyst to obtain the corresponding [4+2] and [4+3] cycloadducts are examined through density functional theory (DFT) calculations at the B3LYP/6-31G* level. The activation effect of LA catalyst can be reached by two ways, that is, interaction of LA either with carbonyl or carboxyl oxygen atoms of **1** to render [4+2] or [4+3] cycloadducts. The *endo* and *exo* [4+2] cycloadducts are formed through a highly asynchronous concerted mechanism associated to a Michael-type addition of **Cp** to the β-conjugated position of α,β-unsaturated carbonyl framework of **1**. Coordination of LA catalyst to the carboxyl oxygen yields a highly functionalized compound, **3**, through a domino reaction. For this process, the first reaction is a stepwise [4+3] cycloaddition which is initiated by a Friedel–Crafts-type addition of the electrophilically activated carbonyl group of **1** to **Cp** and subsequent cyclization of the corresponding zwitterionic intermediate to yield the corresponding [4+3] cycloadduct. The next rearrangement is the nucleophilic trapping of this cycloadduct by a second molecule of **Cp** to yield the final adduct **3**. A new reaction pathway for the [4+3] cycloadditions emerges from the present study.

Keywords: cycloaddition · density functional calculations · Lewis acids · reaction mechanisms

Introduction

The Diels–Alder (DA) reaction between cyclopentadiene (**Cp**), and α,β-unsaturated carbonyl derivatives catalyzed by Lewis acids (LAs) is of wide interest in organic synthesis.[1] In particular, this cycloaddition is taken as reference to evaluate new chiral LAs.[2] Avenoza et al.[3] studied the LA catalyzed ($AlCl_3$, 0.50 equiv) DA reaction between the arylidenoxazolone **1** and **Cp** to yield the *endo* and *exo* [4+2] cycloadducts **2a** and **2b** (see Scheme 1). In further investigations, the authors found that the use of more than 1 equiv $AlCl_3$ or $AlCl_2Et$ as LA catalysts (up to 1.50 equiv) the reaction also afforded product **3** (see Scheme 1).[4] Formation of **3** was explained by means of a domino reaction which is initiated by a [4+3] cycloaddition between an allyl cation, resonance structure **A**, and **Cp** to give the corresponding cycloadduct, structure **B** in Scheme 2, which quickly experiments

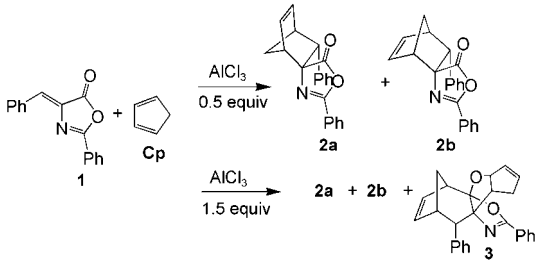

Scheme 1. Reaction studied in this work.

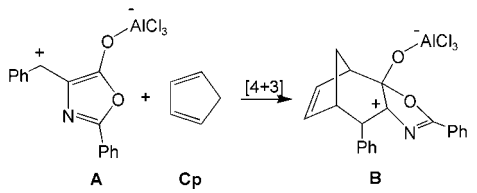

Scheme 2. **B** is the proposed adduct formed by means of a [4+3] cycloaddition between **A** and **Cp**.[4]

[a] Prof. Dr. M. Arnó, Prof. Dr. M. T. Picher, Prof. Dr. L. R. Domingo
Instituto de Ciencia Molecular
Departamento de Química Orgánica
Universidad de Valencia, Dr. Moliner 50
46100 Burjassot, Valencia (Spain)
Fax: (+34) 96-354-3152
E-mail: domingo@utopia.uv.es

[b] Prof. Dr. J. Andrés
Departament de Ciències Experimentals
Universitat Jaume I, Apartat 224
12080 Castelló (Spain)

Supporting information for this article is available on the WWW under http://www.chemeurj.org/ or from the author.

DOI: 10.1002/chem.200400277

a highly regioselective and stereoselective nucleophilic trapping with the excess of **Cp** to give **3**. The scope of this new reaction was tried with other (*Z*)-4-arylidene-2-phenyl-5(4*H*)-oxazolone systems. The reaction of substituted-phenyl systems such as *para*-chloro, -nitro, -bromo or *ortho*-nitro led to the corresponding bicyclo[3.2.1]octane. In the case of the *para*-bromo-oxazolone an excellent yield was obtained for the [4+3] cycloadduct.[4] The extention of this reactivity to other less reactive dienes, such as 2,3-dimethyl-1,3-butadiene or 1,3-cyclohexadiene was also examined, but only a [4+2] cycloaddition was observed in these cases.[4]

The direct construction of seven-membered rings via [4+3] cycloadditions is the most attractive strategy for preparing this frequently observed natural product substructure.[5] Therefore, a great amount of effort has been focused on methods to synthesize the less accessible three-atom component of these reactions[6,7] and in particular, oxyallyl cations are the most employed intermediates to generate this moiety.[6] Alternatively, the use of 2-(silyloxy)acroleins and related compounds in presence of a LA catalyst as the three-atom component in the [4+3] cycloadditions has received much interest in the last years.[7] In the course of the writing the final version of this paper, Davies and Dai[8] have reported the [4+3] cycloaddition between 2-alkylacroleins and **Cp** in presence on 1.1 equiv $AlCl_3$ (see Scheme 3). For 2-methylacrolein, **4**, these authors found that at lower temperatures, that is −78 °C, the reaction yields the *endo* and *exo* [4+2] cycloadducts. When the reaction was allowed to warm to 0 °C [4+3] cycloadduct **6** was the major product with a large diastereoselectivity (96% *de*) (see Scheme 3). These authors proposed a tandem DA reaction/ring expansion for the formation of the [4+3] cycloadduct **6**.[8]

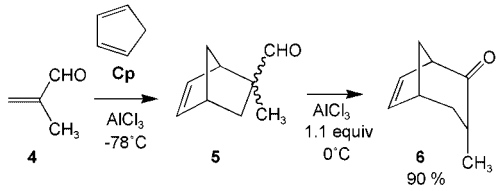

Scheme 3. [4+3] cycloaddition between 2-alkylacroleins and **Cp** reported by Davies and Dai.[8]

The computational approach is very appealing in this field, given the diversity and the difficulties of the experimental elucidation of the corresponding synthetic routes. The mechanism of the [4+3] cycloaddition reaction between 2-hydroxyallyl cations and 1,3-butadiene has been theoretically studied by Cramer and Barrow (see mechanism A in Scheme 4).[9] This reaction takes place through a stepwise mechanism and the first step is the electrophilic attack of the 2-hydroxyallyl cation on the diene to give a cation intermediate, **IN-A**, which by a subsequent ring-closure process affords the final [4+3] cycloadduct. For the intramolecular [4+3] cycloadditions between hydroxyallyl cations and furan a stepwise-like mechanism has been predicted by Harmata and Schreiner,[10] while the *endo*/*exo* preferences involving the cyclopentenyl cation have been explained through a concerted process.[11]

More recently, we have studied the mechanism of the LA catalyzed [4+3] cycloaddition reaction between 2-(silyloxy)-acrolein and furan (see mechanism B in Scheme 4).[12] This reaction is a three-step process that is initialized by the nucleophilic attack of furan to the β-conjugated position of the LA coordinated 2-(silyloxy)acrolein to give a zwitterionic intermediate, **IN1-B**. The key step on the formation of the seven-membered ring is the electrophilic attack of the furan residue to the nucleophilically activated carbonyl carbon at this intermediate, via **TS2-B**.[12] Formation of the final [4+3] cycloadduct requires a silyl migration.

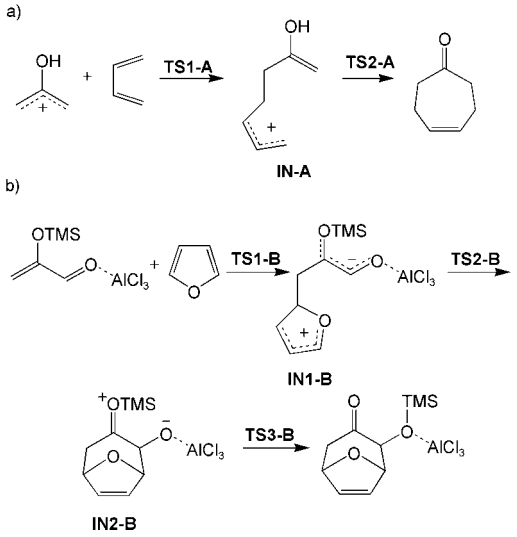

Scheme 4. a) Stepwise mechanism for the [4+3] cycloaddition between 2-hydroxyallyl cation and 1,3-butadiene. b) Stepwise mechanism for the LA catalyzed [4+3] cycloaddition between 2-(silyloxy)acrolein and furan.

In the present work, the reactions between arylidene-5(4*H*)-oxazolone **1**, and **Cp** in absence and in presence of LA, AlH_3, have been studied (see Scheme 5). Our aim was to characterize the nature of the molecular mechanism for the formally [4+3] cycloaddition involved in the formation of the bicyclo[3.2.1]octane framework present in **3**. An effort is made to explain the observed trends from the detailed analysis of the potential energy surface (PES), location and characterization of transition structures (TSs) and related minima. The article is structured as follows: The computational techniques and methodologies adopted are elaborated in the next section together with a brief theoretical background of the global electrophilicity indicator. Next, the results are presented and discussed on the basis of the generated trends in terms of global electrophilicity indexes and the analysis of stationary points on PES. This analysis allows us to rationalize and to explain the experimental observations. Finally, in the concluding section, the net outcome of the work is summarized.

Computational Methods

Density functional theory calculations have been carried out using the B3LYP[13] exchange-correlation functionals, together with the standard 6-31G* basis set.[14] The optimizations were carried out using the Berny analytical gradient optimization method.[15] The stationary points were characterized by frequency calculations in order to verify that the TSs have one and only one imaginary frequency. The intrinsic reaction coordinate (IRC)[16] path was traced in order to check the energy profiles connecting each TS to the two associated minima of the proposed mechanism by using the second order González-Schlegel integration method.[17] The electronic structures of stationary points were analyzed by the natural bond orbital (NBO) method.[18] All calculations were carried out with the Gaussian 98 suite of programs.[19] Cartesian coordinates of all stationary points are given in Supporting Information.

Solvent effects have been considered by B3LYP/6-31G* single point calculations over the gas phase optimized structures using a self-consistent reaction field (SCRF)[20] based on the polarizable continuum model (PCM) of the Tomasi group.[21] We have selected the dielectric constant of dichloromethane, $\varepsilon = 8.93$.

The computed values of enthalpies, entropies and free energies were estimated by means of the B3LYP/6-31G* potential energy barriers, along with the gas-phase harmonic frequencies.[14] A scaling factor[22] of 0.96 for the vibrational energies was used. Thermal corrections to enthalpy and entropy values were evaluated at the experimental temperature of 248.15 K.[4] To calculate enthalpy and entropy at that temperature, the difference between the values at the temperature and 0 K was evaluated according to standard thermodynamics.[23]

The global electrophilicity index, ω,[24] which measures the stabilization energy when the system acquires an additional electronic charge ΔN from the environment, has been given by the following simple expression,[24] $\omega = (\mu^2/2\eta)$, in terms of the electronic chemical potential μ and the chemical hardness η. Both quantities may be approached in terms of the one electron energies of the frontier molecular orbital HOMO and LUMO, ε_H and ε_L, as $\mu \approx (\varepsilon_H + \varepsilon_L)/2$ and $\eta \approx (\varepsilon_L - \varepsilon_H)$, respectively.[25]

Results and Discussion

Firstly, a DFT analysis based on the reactivity indexes of the reagents involved in these cycloadditions will be performed. Then, the [4+2] cycloaddition between the arylidenoxazolone system, **1**, and **Cp** in absence of LA catalyst has been considered in the second section (see Scheme 5a). Later, the presence of LA catalyst has been taken into account; two modes of coordination of LA catalyst with **1** have been considered (see Scheme 5). In **7** the coordination is at the carbonyl oxygen while in **9** it takes place with the carboxyl oxygen. In the second section, the [4+2] cycloaddition between **7** and **Cp** to yield the *endo*, **8a**, and *exo*, **8b**, cycloadducts will also be studied (see Schemes 5b and 6). In the last section the [4+3] cycloaddition between the LA coordinated arylidenoxazolone **9** and **Cp** to give the adduct **10** will be considered (see Schemes 5c and 7).

Global electrophilicity analysis: Recent studies devoted to Diels–Alder[26] and 1,3-dipolar cycloaddition[27] reactions have shown that the global indexes defined in the context of density functional theory[25,28] are a powerful tool to understand the behavior of polar cycloadditions. The difference of global electrophilicity[26] between the reagent pair, $\Delta\omega$, can be used to predict the polar character of the process and thereby the feasibility of the cycloaddition. In Table 1 the static global properties: electronic chemical potential, μ, chemical hardness, η, and global electrophilicity, ω, of arylidene-5(4*H*)-oxazolone, **1**, the corresponding LA coordinated oxazolones, and **Cp** are presented.

Table 1. HOMO and LUMO energies, electronic chemical potential (μ), chemical hardness (η) and global electrophilicity (ω), of the arylidenoxazolones **1** in absence and in presence of the LA catalysts, and **Cp**.

	HOMO [au]	LUMO [au]	μ [au]	η [au]	ω [eV]
12 ($AlCl_3$)	−0.2541	−0.1366	−0.1954	0.1176	4.42
13 ($AlClMe_2$)	−0.2248	−0.1249	−0.1749	0.0999	4.16
7	−0.2377	−0.1211	−0.1794	0.1165	3.76
9	−0.2342	−0.1077	−0.1710	0.1265	3.14
10	−0.2324	−0.1040	−0.1682	0.1284	3.00
1	−0.2184	−0.0912	−0.1548	0.1273	2.56
Cp	−0.2115	-0.0099	−0.1107	0.2016	0.83

The values of the electronic chemical potentials, μ, given in Table 1, indicate that the arylidenoxazolones present a μ lesser than that for **Cp**. Therefore, the charge transfer will take place from **Cp** acting as nucleophile toward the arylidenoxazolone system acting as electrophile (see below). An analysis of the electrophilicity of the arylidenoxazolones given in Table 1 allows us to obtain the following conclusions: i) The electrophilicity of the arylidenoxazolone **1** is 2.56 eV, a value that falls in the range of strong electrophiles within the ω scale.[26] ii) Coordination of LA AlH_3 to the car-

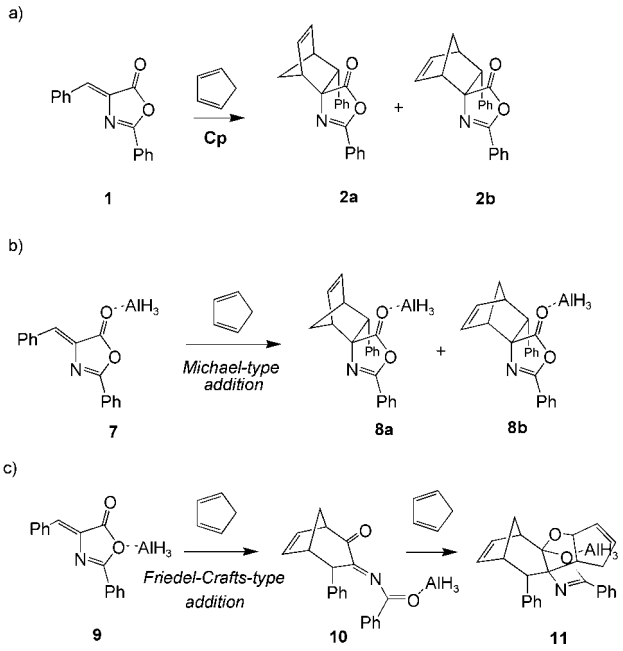

Scheme 5. a) Non-catalyzed [4+2] cycloaddition between **1** and **Cp**. b) Coordination of the LA to the carbonyl oxygen atom of **1**. c) Coordination of the LA to the carboxyl oxygen atom of **1**.

bonyl O1 oxygen of **1** increases the electrophilicity of **7** to 3.76 eV. This fact increases the $\Delta\omega$ for the LA catalyzed [4+2] cycloaddition, and a reduction of the activation energy will be expected along a more polar process (see below). iii) Substitution of the LA AlH_3 in **7** by $AlCl_3$ or $AlClMe_2$, **12** and **13** in Table 1, increases the electrophilicity of **7** to 4.42 and 4.16 eV, respectively, in agreement with the larger acid character of $AlCl_3$ and $AlClMe_2$. A similar trend has been observed for the LA catalyzed [4+2] cycloaddition between nitroethylene and methyl vinyl ether.[29] There is a correlation between electrophilicity of the LA coordinated nitroethylene and the acid character of the LA catalyst, following the order: $AlH_3 < AlMe_3 < AlCl_3$, with concomitant decreasing of the activation barrier, but it does not modify the concerted mechanism.[29] These results allow us to assert the use of AlH_3 as a computational model for the LAs used in the experiments, $AlCl_3$ and $AlClEt_2$.[4]

Study of the [4+2] cycloaddition between aryliden-5(4*H*)-oxazolone, 1, and Cp, in the absence and presence of a LA catalyst: The [4+2] cycloadditions between the arylidenoxazolone **1** (absence of LA) or **7** (presence of LA) and **Cp** can take place along two stereoisomeric reactive channels, the *endo* and *exo* (see Schemes 5 and 6). Experimentally, the two cycloadducts are formed in a 53:47 ratio which indicates that these cycloadditions proceed with a very low stereoselectivity.[4] The two studied reactive channels are associated to the *endo* and *exo* approach modes of **Cp** relative to the carbonyl group of **1** and **7**. An analysis of the gas phase results indicates that these cycloadditions take place along a concerted processes. Therefore four TSs, **TSa-nc**, **TSb-nc**, **TSa** and **TSb**, and four cycloadducts, **2a**, **2b**, **8a** and **8b**, associated to the *endo* and *exo* reactive channels, named as **a** and **b**, for the non-catalyzed, named as **nc**, and LA catalyzed processes, respectively, have been located and characterized. In Scheme 6 the atom numbering is presented while the energetic results are listed in Table 2. The optimized geometries of the TSs are depicted in Figure 1, while the geometry of the cycloadducts are given in Supporting Information.

The activation enthalpies for the non catalyzed and LA catalyzed cycloadditions are: 22.5 (**TSa-nc**), 21.6 (**TSb-nc**), 15.8 (**TSa**) and 15.3 kcal mol^{-1} (**TSb**). Therefore, coordination of the LA to the carbonyl O1 oxygen decreases the activation enthalpy for the catalyzed cycloaddition in about 7 kcal mol^{-1}. Both noncatalyzed and catalyzed processes present a very low stereoselectivity in clear agreement with the experimental results. Inclusion of the activation entropy arises the activation free energy to 34.0 (**TSa-nc**), 33.0 (**TSb-nc**), 27.8 (**TSa**) and 27.2 (**TSb**) kcal mol^{-1}, as a consequence of the negative activation entropy associated of these [4+2] cycloadditions: in the range of −46.1 and −48.4 cal mol^{-1} K^{-1}. Inclusion of solvent effects decreases the relative energies of the TSs between 1.5 and 2.6 kcal mol^{-1}. In addition, solvent effects decrease the stereoselectivity of the LA catalyzed process by a larger solvatation of **TSa** than **TSb**.

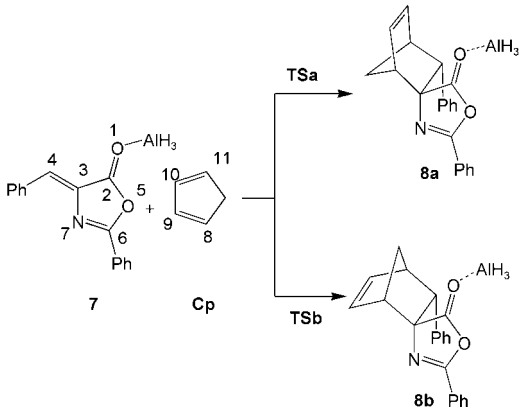

Scheme 6. [4+2] cycloaddition reaction of **7** with **Cp**.

The lengths of the C3–C11 and C4–C8 forming bonds at the TSs are: 2.633 and 1.913 Å at **TSa-nc**, 2.738 and 1.907 Å at **TSb-nc**, 3.221 and 1.887 Å at **TSa**, and 2.961 and 1.915 Å at **TSb**, respectively, while the corresponding bond order (BO) values[30] are: 0.19 and 0.58 at **TSa-nc**, 0.16 and 0.57 at **TSb-nc**, 0.00 and 0.60 at **TSa**, and 0.09 and 0.56 at **TSb**, respectively. These BO values indicate that these TSs correspond to highly asynchronous bond-formation processes, while for the LA catalyzed reaction the TSs correspond to two-center additions. Therefore, the nucleophilic attack of **Cp** to the β position of the LA coordinated α,β-unsaturated carbonyl moiety of **7** can be associated to a Michael-type addition.[31] In spite of the high asynchronicity found at the

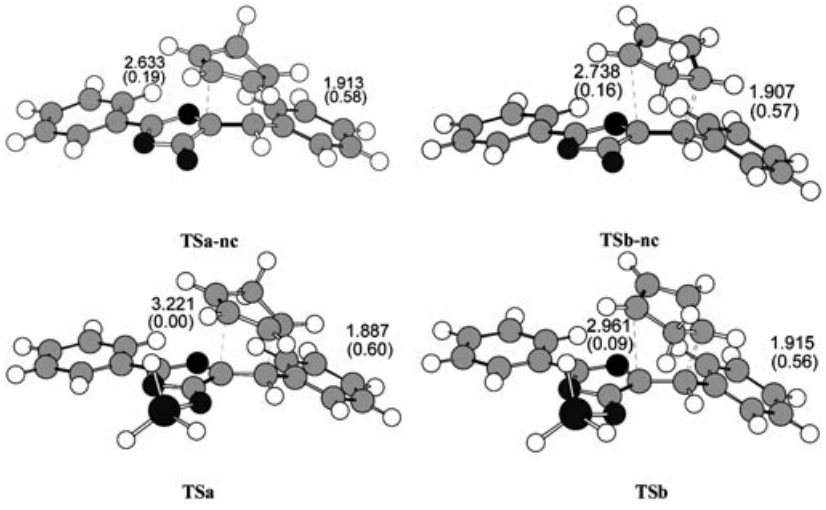

Figure 1. Optimized geometries of the transition structures for the *endo*, **TSa-nc**, and *exo*, **TSb-nc**, channels of non-catalyzed reaction between **1**, and **Cp**. **TSa** and **TSb** are the transition structures for the reaction between **7** and **Cp**. In **7** the LA (AlH_3) catalyst is coordinated to the carbonyl oxygen atom of **1**. The distances directly involved in the bond-forming processes are given in angstroms. Bond order values are given in parenthesis.

Table 2. Relative energies[a] (ΔE, kcal mol^{-1}), enthalpies (ΔH, kcal mol^{-1}), entropies (ΔS, cal mol^{-1} K^{-1}) and free energies (ΔG, kcal mol^{-1}) in vacuum at 248.15 K and 1 atm, and relative energies in dichloromethane (ΔE_{sol}, kcal mol^{-1}) corresponding to the stationary points of the reactions of the phenylidenoxazolones **1**, **7** and **9** with **Cp**.

	ΔE	ΔH	ΔS	ΔG	ΔE_{sol}
a) [4+2] cycloaddition between **1** and **Cp**					
TS a-nc	21.6	22.5	−46.3	34.0	19.9
TS b-nc	20.8	21.6	−46.1	33.0	19.3
2a	−2.6	0.3	−49.2	12.5	−3.0
2b	−3.6	−0.5	−50.5	12.0	−3.8
b) LA catalyzed [4+2] cycloaddition between **7** and **Cp**					
TS a	14.8	15.8	−48.4	27.8	12.2
TS b	14.5	15.3	−47.9	27.2	12.2
8a	−2.3	0.6	−50.5	13.2	−2.6
8b	−2.6	0.4	−51.3	13.1	−2.9
c) LA catalyzed [4+3] cycloaddition between **9** and **Cp**					
TS1	19.9	20.1	−45.5	31.4	13.8
IN1	17.7	18.7	−41.9	29.1	9.5
TS2	19.4	20.2	−50.5	32.7	14.1
10	−13.2	−10.3	−45.6	1.0	−18.0
TS3	6.9	10.5	−98.3	34.9	1.7
11	−20.5	−13.9	−103.9	11.8	−21.6

[a] Relatives to **Cp** and the corresponding phenylidenoxazolones **1**, **7** and **9**.

TSs of the LA catalyzed process, the IRC analysis establishes the one-step nature of these cycloadditions.

The natural population analysis (NPA)[18a] allows the evaluation of the charge transfer (CT) along these [4+2] cycloaddition processes. The B3LYP/6-31G* atomic charges at the TSs have been partitioned between **Cp** and the arylidenoxazolone frameworks. The values of negative charges transferred from the donor **Cp** to the arylidenoxazolone moiety are: 0.25 e (**TS a-nc**), 0.24 e (**TS b-nc**), 0.38 e (**TS a**), and 0.37 e (**TS b**), thereby indicating that the nature of these TSs may be traced to some zwitterionic character. The CT at the LA catalyzed processes is larger than that at the non catalyzed ones. This is in agreement the increase of $\Delta\omega$ associated to the catalyzed process (see first section of Results and Discussion). The LA increases the electrophilicity of the arylidenoxazolone **1** favoring the cycloaddition through a more polar process. Incorporation of solvent effects on the NBO calculations increases the CT at these polar TSs: 0.30 e (**TS a-nc**), 0.28 e (**TS b-nc**), 0.44 e (**TS a**), and 0.43 e (**TS b**). This behavior can be explained by a larger stabilization of the corresponding zwitterionic TSs that allows a larger CT.[32]

Study of the [4+3] cycloaddition between LA coordinated arylidenoxazolone 9 and Cp: Oxyallyl cations experiment nucleophilic addition at both allylic positions.[9] On the other hand, the LA coordinates α,β-unsaturated carbonyl derivatives as **7** experiment nucleophilic addition at the electrophilically activated β position (the C4 carbon).[12,31] In the case of the LA coordinated arylidenoxazolone **7** all attempts for the direct addition of **Cp** to the carbonyl C2 carbon of **7** failed. In addition, all attempts to form a seven-membered cycloadduct after **TS a** and **TS b**, second step on the mechanism (B) in Scheme 4, or interconversion of the [4+2] cycloadducts **8a** and **8b** into the [4+3] cycloadduct **10** through a ring expansion, were also unsuccessful. Therefore, the participation of the C2-C3-C4 framework of **1** as the three-atom component in the formation of the seven-membered ring requires a strong electrophilic activation of the carbonyl group. Viewing the C2(=O1)−O5−C6=N7 framework of **1** as an aza analogue of an acid anhydride this activation could be achieved by coordination of the LA catalyst to the carboxyl O5 oxygen of the arylidenoxazolone **1**. This coordination, presented in **9**, opens an alternative reactive channel, as it is depicted in Schemes 5c and 7. Therefore, the electrophilic attack of the activated acyl carbon of **9** to **Cp** could yield the [4+3] cycloadduct **10** via an initial Friedel–Crafts-type addition to olefins.[33]

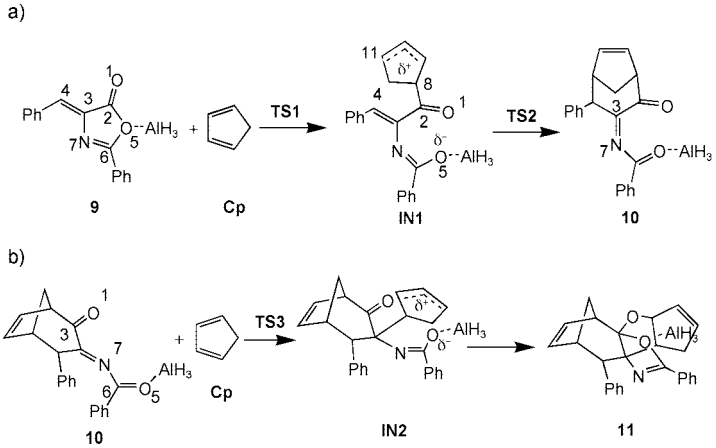

Scheme 7. Domino reaction between **9** and excess of **Cp**. a) [4+3] cycloaddition between **9** and **Cp**. b) Nucleophilic capture of **10** with excess **Cp**.

The reaction between the LA coordinated arylidenoxazolone **9** and excess of **Cp** to give the bicyclo[3.2.1]octane adduct **11** involves two consecutive reactions (see Scheme 5c and 7). The first one corresponds to a stepwise [4+3] cycloaddition with formation of the seven-membered ring, while the second one is a formally [3+2] cycloaddition between the [4+3] cycloadduct **10** and a second molecule of **Cp** with concomitant formation of the oxa five-membered ring, **11**.

An exhaustive exploration of the PES for the [4+3] cycloaddition between the LA activated arylidenoxazolone **9** and **Cp** to yield the cycloadduct **10** renders two TSs, **TS1** and **TS2**, and one intermediate, **IN1**. The first step of this [4+3] cycloaddition is the electrophilic attack of the carbonyl C2 carbon of the oxazolone **9** to **Cp**, via **TS1**, to give the zwitterionic intermediate **IN1**. The second step corresponds to the cyclization of this intermediate, via **TS2**, with formation of the seven-membered ring. The different stationary points for the stepwise [4+3] cycloaddition between **9** and **Cp** are

depicted in Scheme 7 together with the atom numbering, while the energetic results are listed in Table 2. The geometries of the TSs are presented in Figure 2, while the geometries of the intermediates and cycloadducts are given in Supporting Information.

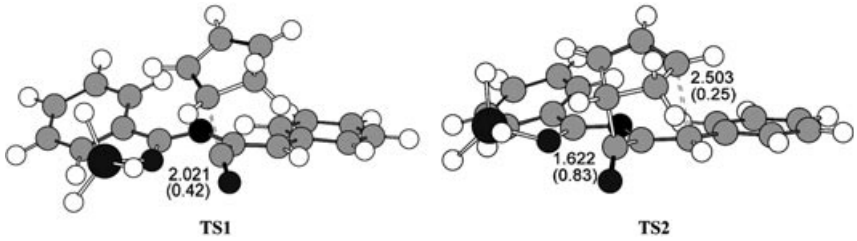

Figure 2. Optimized geometries of the transition structures, **TS1** and **TS2**, for the stepwise [4+3] cycloaddition reaction between **Cp** and **9**. In **9** the LA (AlH_3) catalyst is coordinated to the carboxyl oxygen atom of **1**. The distances directly involved in the bond-forming processes are given in Ångstroms. Bond order values are given in parenthesis.

The first electrophilic attack, which corresponds to a Friedel–Crafts-type addition of the carbonyl C2 carbon of **9** to the π system of **Cp**, presents an activation enthalpy of 20.1 kcal mol^{-1}. Inclusion of the activation entropy, −45.5 cal mol^{-1} K^{-1}, arises the activation free energy to 31.4 kcal mol^{-1}. Solvent effects cause a large reduction of the gas phase activation energy, 6.1 kcal mol^{-1}. This reduction is larger than that for the nucleophilic attack of **Cp** to **7**, 2.6 kcal mol^{-1}. Therefore, in condensed phase the activation free energies for the Michael-type addition of **Cp** to **7** and the Friedel–Crafts-type addition of **9** to **Cp** could be closer, being both reactive channels competitive. The free energy associated to the formation of the intermediate **IN1** is 29.1 kcal mol^{-1}. The subsequent cyclization step presents an activation enthalpy of 1.5 kcal mol^{-1} and formation of the bicyclo[3.2.1]octane adduct **10** is exothermic, −10.3 kcal mol^{-1}. With the inclusion of solvent effects the adduct **10** stabilizes in 5.2 kcal mol^{-1} relative to the gas phase results as a consequence of its large polar character.

The length of the C2–C8 forming bond at **TS1** is 2.021 Å, while the C4–C11 and C2–O5 distances are 3.538 and 2.237 Å, respectively. Along the electrophilic attack of **9** to **Cp**, the oxazolone ring is opened with concomitant C2–O5 bond-breaking process. At the intermediate **IN1** the C2–C8 bond length, 1.672 Å, indicates that this bond is already formed, while the C2–O5 distance increases to 2.877 Å. At **TS2**, the C4–C11 bond length is 2.503 Å while the C2–O5 distance is 2.460 Å. At the [4+3] cycloadduct **10** the lengths of the C2–C8 and C4–C11 bonds are 1.519 and 1.565 Å, respectively; this indicates that these bonds are already formed, while the C2–O5 distance is 3.292 Å. These results support the cleavage of the oxazolene ring in **10**. The BO values of the C2–C8 forming bond at **TS1** and **TS2** are 0.42 and 0.83, respectively, while the C4–C11 BO at **TS2** is 0.25. The C3–N7 BO value at the [4+3] cycloadduct **10** is 1.82, which indicates that it has a double-bond character. Therefore, the C3=N7–C6(Ph)=O5 framework of the [4+3] cycloadduct **10** corresponds to a N-acyl imine. Coordination of the LA AlH_3 to the O5 oxygen increases the electrophilicity of the imine C3 carbon, allowing to explain the reactivity of **10** toward the nucleophilic addition of **Cp**. This electrophilic activation is in agreement by the large electrophilicity of the [4+3] cycloadduct **10**, 3.00 eV, which is closer to that for the LA coordinated arylidenoxazolone **9** (see Table 1).

The negative charge transferred from the donor **Cp** to the arylidenoxazolone **9** along the electrophilic attack of the carbonyl C2 carbon of **9** to **Cp** is 0.33 e at **TS1**, 0.60 e at **IN1** and 0.35 e at **TS2**, thereby indicating the large polar nature of this [4+3] cycloaddition. The CT at **TS1**, associated to the Friedel–Crafts-type addition, is slightly less than that found at **TS a** (0.38 e), associated to the Michael-type addition, in agreement with the lower electrophilicity of the LA coordinated arylidenoxazolone **9** than the **7** one (see Table 1). Incorporation of solvent effects on the NBO calculations increases the CT of the stationary points associated to the Friedel–Crafts-type addition to 0.39 e at **TS1**, 0.66 e at **IN1**, and 0.41 e at **TS2**.

One of the referees proposed to consider the coordination of LA to the nitrogen of the oxazolone ring (see **14** in Scheme 8). This coordination gives a stepwise mechanism for the [4+3] cycloaddition like that for attack of **Cp** to **9**. However, although the LA coordinated oxazolone **14** is 9.0 kcal mol^{-1} more stable than **9**, the activation energy associated to the nucleophilic attack of **Cp** to **14** presents a high value, 31.5 kcal mol^{-1}. This unfavorable barrier allows to discard the mechanism given in Scheme 8. The total electronic energies, the geometries and the Cartesian coordinates of **14** and **TS4** are given in Supporting Information.

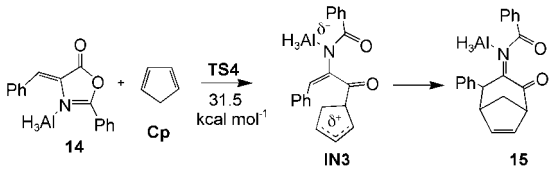

Scheme 8. [4+3] cycloaddition reaction between **14** and **Cp**.

The second reaction is a formally [3+2] cycloaddition between the [4+3] cycloadduct **10** and a second molecule of **Cp**, followed by a ring closure with formation of the oxazolone system to give the final cycloadduct **11** (see Scheme 7). An exhaustive exploration of the PES for this reaction allows to find only one TS, **TS3**, associated to the nucleophilic attack of **Cp** to the electrophilically activated imine C3 carbon of the [4+3] cycloadduct **10**. The activation enthalpy associated with **TS3** is 20.8 kcal mol^{-1}. After **TS3**, the intermediate and TSs associated with the formation of the

final cycloadduct **11** are located in a smooth drop energy after the barrier height. This fact precludes the localization of the corresponding stationary points. However, the IRC from **TS3** to the cycloadduct stops at a structure that lies 4.0 kcal mol^{-1} below **TS3** (see **IN2** in Scheme 7). The total electronic energy and the Cartesian coordinates of **IN2** are given in Supporting Information. The ring closure process at these species with formation of the O1−C9 bond presents a very low barrier; it has been estimated at less of 0.5 kcal mol^{-1}. The C2−O5 bond-formation process with regeneration of the oxazolone ring takes place after the formation of the O1−C9 bond. The formally [3+2] cycloaddition is slightly endothermic in 0.13 kcal mol^{-1}. Therefore, the domino reaction between **9** and **Cp** with formation of **11** is exothermic, −13.9 kcal mol^{-1}.

The length of the C3−C8 bond forming at **TS3** is 2.063 Å, while the O1−C11 distance is 2.768 Å (see Figure 3). The C2−O5 distance, 2.559 Å, indicates that the oxazolone ring remains open at this step. The BO value of the C3−C8 bond at **TS3** is 0.45. The negative charge transferred from the donor **Cp** to the [4+3] cycloadduct **10** at **TS3** is 0.40 e, in accordance with the large polar character of the process. This large CT is in agreement with large electrophilicity of **10** (see Table 1). Incorporation of solvent effects on the NBO calculations increases the CT of **TS3** to 0.43 e.

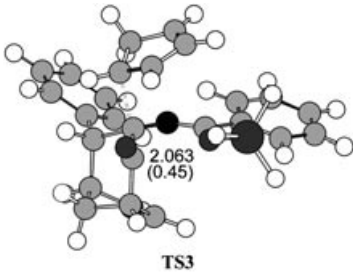

Figure 3. Optimized geometries of the transition structure, **TS3**, corresponding to the nucleophilic attack of **Cp** to the C3 carbon atom of the [4+3] cycloadduct intermediate **10**. The distance directly involved in the bond-forming process is given in Ångstroms. Bond order value is given in parenthesis.

Conclusion

The molecular mechanisms of the reactions between aryliden-5(4*H*)-oxazolone, **1**, and **Cp** in absence and in presence of LA catalyst have been studied at B3LYP/6-31G* computing level. In absence of LA, the [4+2] cycloaddition takes place through a concerted mechanism. Presence of the LA coordinated to the carbonyl oxygen of **1** accelerates the [4+2] cycloaddition through a highly asynchronous polar TS. This catalyzed process can be associated to a Michael-type addition of **Cp** to the β-conjugated position of the arylidenoxazolone followed by a concomitant cyclization. These [4+2] cycloadditions do not exhibit *endo*/*exo* selectivity.

A new mechanism emerges from this DFT study for the [4+3] cycloaddition. This requires the strong electrophilic activation of the carbonyl carbon of the α,β-unsaturated carboxyl moiety of the aryliden-5(4*H*)-oxazolone **1** in order to work this conjugated system as the three-atom component of a [4+3] cycloaddition. This activation, which has been modeled by coordination of the LA to the carboxyl oxygen, renders a Friedel–Crafts-type addition to the diene component of **Cp** to give a zwitterionic intermediate that by a subsequent cyclization yields the seven-membered cycloadduct.

Finally, coordination of the LA to the N-acyl imine framework present on the [4+3] cycloadduct increases its electrophilicity, being then trapped with the excess of **Cp** to give the adduct **3**.

Acknowledgments

This work was supported by research funds provided by the Ministerio de Educación y Cultura of the Spanish Government by DGICYT (project BQU2002–01032), and by the Agencia Valenciana de Ciencia y Tecnología of the Generalitat Valenciana (reference GRUPOS03/176). All calculations were performed on a Cray-Silicon Graphics Origin 2000 of the Servicio de Informática de la Universidad de Valencia.

[1] a) E. J. Corey, A. Guzman-Perez, *Angew. Chem.* **1998**, *110*, 402–415; *Angew. Chem. Int. Ed.* **1998**, *37*, 388–401; b) K. Ishihara, H. Yamamoto, *Eur. J. Org. Chem.* **1999**, 527–538; c) E. J. Corey, *Angew. Chem.* **2002**, *114*, 1724–1741; *Angew. Chem. Int. Ed.* **2002**, *41*, 1650–1667.

[2] a) K. Ishihara, H. Kurihara, M. Matsumoto, H. Yamamoto, *J. Am. Chem. Soc.* **1998**, *120*, 6920–6930; b) J. W. Faller, B. J. Grimmond, D. G. D'Alliessi, *J. Am. Chem. Soc.* **2001**, *123*, 2525–2529; c) E. J. Corey, T. Shibata, T. W. Lee, *J. Am. Chem. Soc.* **2002**, *124*, 3808–3809.

[3] a) A. Avenoza, C. Cativiela, M. González, J. A. Mayoral, M. A. Roy, *Synthesis* **1990**, 1114–1116; b) A. Avenoza, C. Cativiela, M.-D. Díaz-de-Villegas, J. A. Mayoral, J. M. Peregrina, *Tetrahedron* **1993**, *49*, 677–684.

[4] A. Avenoza, J. H. Busto, C. Cativiela, J. M. Peregrina, *Tetrahedron Lett.* **2002**, *43*, 4167–4170.

[5] a) R. Noyori, Y. Hayakawa, *Org. React.* **1983**, *29*,163–344; b) H. M. R. Hoffmann, *Angew. Chem.* **1984**, *96*, 1–16; *Angew. Chem. Int. Ed. Engl.* **1984**, *23*, 1–19; c) A. Hosomi, Y. Tominaga, *Comprehensive Organic Synthesis*, *Vol. 5* (Eds.: B. M. Trost, I. Fleming), Pergamon, Oxford, **1991**, pp. 593–615; d) M. Harmata, *Tetrahedron* **1997**, *53*, 6235–6280.

[6] a) J. Mann, *Tetrahedron* **1986**, *42*, 4611–4659; b) J. K. Cha, J. Oh, *Curr. Org. Chem.* **1998**, *2*, 217–232; c) M. Harmata, D. E. Jones, M. Kahraman, U. Sharma, C. Barnes, *Tetrahedron Lett.* **1999**, *40*, 1831–1834; d) A. A. O. Sarhan, *Curr. Org. Chem.* **2001**, *5*, 827–844; e) M. Harmata, G. J. Bohnert, *Org. Lett.* **2003**, *5*, 59–61.

[7] a) T. Sasaki, Y. Ishibashi, M. Ohno, *Tetrahedron Lett.* **1982**, *23*, 1693–1696; b) C. Blackburn, R. F. Childs, R. A. Kennedy, *Can. J. Chem.* **1983**, *61*, 1981–1986; c) M. Harmata, U. Sharma, *Org. Lett.* **2000**, *2*, 2703–2705; d) R. A. Aungst Jr., R. L. Funk, *Org. Lett.* **2001**, *3*, 3553–3555.

[8] H. M. Davies, X. Dai, *J. Am. Chem. Soc.* **2004**, *126*, 2692–2693.

[9] a) C. J. Cramer, S. E. Barrow, *J. Org. Chem.* **1998**, *63*, 5523–5532; b) C. J. Cramer, S. E. Barrow, *J. Phys. Org. Chem.* **2000**, *13*, 176–186.

[10] M. Harmata, P. R. Schreiner, *Org. Lett.* **2001**, *3*, 3663–3665.

[11] C. J. Cramer, M. Harmata, P. Rashatasakhon, *J. Org. Chem.* **2001**, *66*, 5641–5644.

[12] J. A. Sáez, M. Arnó, L. R. Domingo, *Org. Lett.* **2003**, *5*, 4117–4120.

[13] a) A. D. Becke, *J. Chem. Phys.* **1993**, *98*, 5648–5652; b) C. Lee, W. Yang, R. G. Parr, *Phys. Rev. B* **1988**, *37*, 785–789.

[14] W. J. Hehre, L. Radom, P. v. R. Schleyer, J. A. Pople, *Ab initio Molecular Orbital Theory*, Wiley, New York, **1986**.

[15] H. B. Schlegel, "Geometry Optimization on Potential Energy Surface" in *Modern Electronic Structure Theory* (Ed.: D. R. Yarkony), World Scientific Publishing, Singapore, **1994**.

[16] K. Fukui, *J. Phys. Chem.* **1970**, *74*, 4161–4163.
[17] a) C. González, H. B. Schlegel, *J. Phys. Chem.* **1990**, *94*, 5523–5527; b) C. González, H. B. Schlegel, *J. Chem. Phys.* **1991**, *95*, 5853–5860.
[18] a) A. E. Reed, R. B. Weinstock, F. Weinhold, *J. Chem. Phys.* **1985**, *83*, 735–746; b) A. E. Reed, L. A. Curtiss, F. Weinhold, *Chem. Rev.* **1988**, *88*, 899–926.
[19] *Gaussian 98*, Revision A.6, M. J. Frisch, G. W. Trucks, H. B. Schlegel, G. E. Scuseria, M. A. Robb, J. R. Cheeseman, V. G. Zakrzewski, J. A. Montgomery, J., R. E. Stratmann, J. C. Burant, S. Dapprich, J. M. Millam, A. D. Daniels, K. N. Kudin, M. C. Strain, O. Farkas, J. Tomasi, V. Barone, M. Cossi, R. Cammi, B. Mennucci, C. Pomelli, C. Adamo, S. Clifford, J. Ochterski, G. A. Petersson, P. Y. Ayala, Q. Cui, K. Morokuma, D. K. Malick, A. D. Rabuck, K. Raghavachari, J. B. Foresman, J. Cioslowski, J. V. Ortiz, B. B. Stefanov, G. Liu, A. Liashenko, P. Piskorz, I. Komaromi, R. Gomperts, R. L. Martin, D. J. Fox, T. Keith, M. A. Al-Laham, C. Y. Peng, A. Nanayakkara, C. Gonzalez, M. W. Challacombe, P. M. Gill, B. Johnson, W. Chen, M. W. Wong, J. L. Andres, C. Gonzalez, M. Head-Gordon, E. S. Replogle, J. A. Pople, Gaussian, Inc., Pittsburgh PA, **1998**.
[20] a) O. Tapia, *J. Math. Chem.* **1992**, *10*, 139–181; b) J. Tomasi, M. Persico, *Chem. Rev.* **1994**, *94*, 2027–2094; c) B. Y. Simkin, I. Sheikhet, *Quantum Chemical and Statistical Theory of Solutions—A Computational Approach*, Ellis Horwood, London, **1995**.
[21] a) M. Cossi, V. Barone, R. Cammi, J. Tomasi, *Chem. Phys. Lett.* **1996**, *255*, 327–335; b) E. Cances, B. Mennuncci, J. Tomasi, *J. Chem. Phys.* **1997**, *107*, 3032–3041; c) V. Barone, M. Cossi, J. Tomasi, *J. Comput. Chem.* **1998**, *19*, 404–417.
[22] A. P. Scott, L. Radom, *J. Phys. Chem.* **1996**, *100*, 16502–16513.
[23] D. A. McQuarrie, J. D. Simon, *Molecular Thermodynamics*, University Science Books, Sausalito, California, **1999**.
[24] R. G. Parr, L. von Szentpaly, S. Liu, *J. Am. Chem. Soc.* **1999**, *121*, 1922–1924.
[25] a) R. G. Parr, R. G. Pearson, *J. Am. Chem. Soc.* **1983**, *105*, 7512–7516; b) R. G. Parr, W. Yang, *Density Functional Theory of Atoms and Molecules*, Oxford University Press, New York, **1989**.
[26] L. R. Domingo, M. J. Aurell, P. Pérez, R. Contreras, *Tetrahedron* **2002**, *58*, 4417–4423.
[27] P. Pérez, L. R. Domingo, M. J. Aurell, R. Contreras, *Tetrahedron* **2003**, *59*, 3117–3125.
[28] P. Geerlings, F. De Proft, W. Langenaeker, *Chem. Rev.* **2003**, *103*, 1793–1873.
[29] L. R. Domingo, A. Asensio, P. Arroyo, *J. Phys. Org. Chem.* **2002**, *15*, 660–666.
[30] K. B. Wiberg, *Tetrahedron* **1968**, *24*, 1083–1096.
[31] L. R. Domingo, J. Andrés, C. N. Alves, *Eur. J. Org. Chem.* **2002**, 2557–2564.
[32] L. R. Domingo, M. Arnó, J. Andrés, *J. Org. Chem.* **1999**, *64*, 5857–5875.
[33] a) B. B. Snider, A. C. Jackson, *J. Org. Chem.* **1982**, *47*, 5393–5395; b) R. Faure, A. Pommier, J.-M. Pons, M. Rajzmann, M. Santelli, *Tetrahedron* **1992**, *48*, 8419–8430.

Received: March 22, 2004
Published online: August 10, 2004

